

Production of supersymmetric particles in elastic ep collisions

M. Drees

*Physics Department, University of Wisconsin, Madison, Wisconsin 53706
and CERN, Geneva, Switzerland*

D. Zeppenfeld

*Physics Department, University of Wisconsin, Madison, Wisconsin 53706
(Received 18 November 1988)*

The reactions $ep \rightarrow p\bar{e}\tilde{Z}_i$ and $ep \rightarrow p\tilde{\nu}\tilde{W}_-$ are investigated, where \tilde{Z}_i and \tilde{W}_- are a generic neutralino and the lightest chargino eigenstate, respectively. We present both exact results and a modified effective-photon approximation. We show that ten fully measured $\bar{e}\tilde{Z}_1$ events with $\bar{e} \rightarrow e\tilde{Z}_1$ decay, where the \tilde{Z}_1 escape detection, are enough to determine $m_{\tilde{e}}$ and $m_{\tilde{Z}_1}$ with statistical errors of 2 GeV; the detection of the outgoing proton in a forward proton spectrometer is crucial. $\bar{e}\tilde{Z}_2$ and $\tilde{\nu}\tilde{W}_-$ production, resulting mostly in final states with one or three charged leptons plus missing p_T , are also discussed. Within the framework of minimal supergravity models, these elastic processes make the DESY ep collider HERA competitive with or even superior to the contemporary colliders CERN LEP I and Fermilab Tevatron as far as searches for supersymmetry are concerned.

I. INTRODUCTION

An important task for any new collider is to search for new physics, i.e., the missing parts of the standard model (SM) such as the top quark or physics beyond the standard model. One of the most attractive extensions of the SM is supersymmetry,¹ since it may allow us to solve the problem of the naturalness² of the SM.

Among the machines that will be running in the next few years, the Fermilab Tevatron³ and LEP⁴ at CERN are usually considered to be most promising as far as searches for supersymmetry are concerned. The most thoroughly investigated^{5,6} supersymmetric processes for ep colliders, such as HERA at DESY, are associated slepton-squark production: $ep \rightarrow \bar{e}\tilde{q}X$ and $ep \rightarrow \tilde{\nu}qX$. The limit of sensitivity for these processes is reached for⁶ $m_{\tilde{q}} + m_{\tilde{e},\tilde{\nu}} \simeq 140\text{--}160$ GeV, whereas the Tevatron should be able³ to detect squarks up to $m_{\tilde{q}} \simeq 150\text{--}180$ GeV and thus cover the whole region where $\tilde{l}\tilde{q}$ production can be detected at HERA. The only other supersymmetric process that has so far been discussed for ep colliders is⁷ the deep-inelastic production of a selectron and a photino, $ep \rightarrow \bar{e}\tilde{\gamma}X$. Based on the fact that after one year (corresponding to an integrated luminosity of 200 pb^{-1}) HERA can only probe the region below⁷ $m_{\tilde{e}} \simeq 45$ GeV even if $m_{\tilde{\gamma}} = 0$ the authors of Ref. 8 concluded that this process is not expected to produce very useful limits.

In this paper we study the *elastic* production⁹ of sleptons and gauginos via the processes $ep \rightarrow \bar{e}\tilde{Z}_i p$ and $ep \rightarrow \tilde{\nu}_e \tilde{W}_- p$, where \tilde{Z}_i and \tilde{W}_- denote a generic neutralino eigenstate and the lightest chargino, respectively. Elastic selectron-photino production is an important special case of the first class of processes considered. In this case we find the cross section for the elastic process to be

very similar to the deep-inelastic one.^{7,10} In general we use the minimal supersymmetric model¹ as an example for "realistic" masses and mixings of the produced gauginos.

Elastic selectron-gaugino production at HERA has several nice features. The potential mass reach is quite high. Even though after one year one can only probe the region below $m_{\tilde{e}}, m_{\tilde{W}_-} \simeq 45\text{--}50$ GeV, this limit can be considerably improved as more data are accumulated, going up to about 80 GeV after 5 years. Furthermore the total cross sections turn out to depend rather mildly on the mass of the neutral superparticle produced. Already after one year HERA can hence probe the region below $m_{\tilde{Z}_i} \simeq 60$ GeV and $m_{\tilde{\nu}} \simeq 70$ GeV if $m_{\tilde{e}} = M_{\tilde{W}_-} = 25$ GeV.

In most cases the final states are very clean and essentially free of background: $\bar{e}\tilde{Z}_1$ production with subsequent $\bar{e} \rightarrow e\tilde{Z}_1$ decay, as well as $\tilde{W}_- \tilde{\nu}_e$ production followed by the decay $\tilde{W}_- \rightarrow \tilde{\nu}_e e$, result in one electron and missing energy/momentum, whereas $\bar{e}\tilde{Z}_2$ production can lead to three charged leptons via $\bar{e} \rightarrow e\tilde{Z}_1, \tilde{Z}_2 \rightarrow l^+ l^- \tilde{Z}_1$.

The energy of the outgoing proton can be measured in a forward proton spectrometer. The center-of-mass energy of the slepton-gaugino system will thus be known. For $e\bar{e}\tilde{Z}_i$ and $e\tilde{\nu}_e \tilde{W}_-$ production at e^+e^- colliders this will only be true around $\sqrt{s} \simeq M_{\tilde{Z}_i}$, where annihilation diagrams are strongly enhanced.^{4,11} At other beam energies the outgoing electron will usually be lost.^{4,12,13} We will see that the measurement of the proton energy greatly simplifies the event reconstruction. In the simplest case of $\bar{e}\tilde{Z}_1$ production ten fully measured events should suffice to determine both $m_{\tilde{e}}$ and $m_{\tilde{Z}_1}$ with an error of about 2 GeV.

The remainder of this paper is organized as follows. In Sec. II we give the exact tree-level cross sections for

$ep \rightarrow \tilde{e}\tilde{Z}_i p$ and $ep \rightarrow \tilde{\nu}_e \tilde{W}_- p$, properly taking into account all form factors of the proton. We also derive a modified equivalent-photon (Weizsäcker-Williams) approximation¹⁴ which reproduces the exact results to better than 30%. In Sec. III we discuss in detail the signal and event reconstruction for the simplest and perhaps most interesting of the processes considered, $\tilde{e}\tilde{Z}_1$ production with $\tilde{e} \rightarrow e\tilde{Z}_1$ decay. In Sec. IV the various signals that can emerge from $\tilde{e}\tilde{Z}_2$ and $\tilde{\nu}_e \tilde{W}_-$ production are discussed. In Sec. V we show how the total cross sections depend on the parameters of the minimal supersymmetric model and try to assess the discovery potential of the HERA collider. Finally, Sec. VI contains our conclusions.

II. FORMALISM

A. Exact cross sections

The Feynman diagrams for $ep \rightarrow \tilde{e}\tilde{Z}_i p$ and $ep \rightarrow \tilde{\nu}_e \tilde{W}_- p$ are shown in Figs. 1 and 2, respectively. From these figures it is obvious that the squared matrix element, averaged/summed over spins, can be factorized in the form

$$\sum |M|^2 = \frac{e^2}{(Q^2)^2} L_{\mu\nu} H^{\mu\nu}, \quad (2.1)$$

$$L_{\tilde{e}}^{\mu\nu} = 8e^4 \left[p_1^\mu p_1^\nu \frac{m^2 - M^2}{\hat{s}^2} + p_2^\mu p_2^\nu \left(\frac{m^2 - M^2}{(\hat{u} - M^2)^2} - \frac{q^2}{\hat{s}(\hat{u} - M^2)} \right) + \frac{1}{4\hat{s}} g^{\mu\nu} \left(\hat{t} - m^2 + \frac{q^2}{\hat{s}}(m^2 - M^2) \right) + \frac{1}{2}(p_1^\mu p_2^\nu + p_2^\mu p_1^\nu) \frac{q^2 + 2(m^2 - M^2)}{\hat{s}(\hat{u} - M^2)} \right]. \quad (2.4)$$

Here terms proportional to q^μ or q^ν have been neglected, since they vanish upon contraction with the hadronic tensor $H_{\mu\nu}$. $m \equiv m_{\tilde{\gamma}}$ and $M = M_{\tilde{e}}$ are the neutralino and the selectron mass, respectively. For a general neutralino state only the prefactor has to be changed (see Sec. IV).

For chargino-sneutrino production we find ($m = m_{\tilde{\nu}_e}$, $M = M_{\tilde{W}_-}$)

$$L_{\tilde{W}_-}^{\mu\nu} = 4 \frac{e^4 f_+^2}{\sin^2 \theta_W} \left[p_1^\mu p_1^\nu \left(\frac{M^2 - m^2}{\hat{s}^2} + \frac{q^2}{\hat{s}(\hat{u} - M^2)} \right) + p_2^\mu p_2^\nu \left(\frac{M^2 - m^2}{(\hat{u} - M^2)^2} + \frac{q^2}{\hat{s}(\hat{u} - M^2)} \right) + \frac{1}{4} g^{\mu\nu} [q^2(M^2 - m^2) + \hat{s}(\hat{u} - M^2)] \left[\frac{1}{\hat{s}} + \frac{1}{\hat{u} - M^2} \right]^2 + (p_1^\mu p_2^\nu + p_2^\mu p_1^\nu) \frac{M^2 - m^2 - q^2}{\hat{s}(\hat{u} - M^2)} \right], \quad (2.5)$$

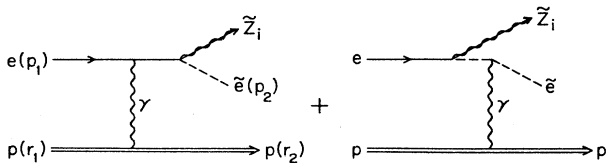


FIG. 1. Feynman diagrams for the process $ep \rightarrow p\tilde{e}\tilde{Z}_i$.

where $H_{\mu\nu}$ describes the photon-proton interaction and $L_{\mu\nu}$ the hard-photon-electron scattering. $H_{\mu\nu}$ is process independent and can conveniently be written in terms of the sum $p = r_1 + r_2$ and the difference $q = r_1 - r_2$ of the momenta of the incoming (r_1) and outgoing (r_2) protons:

$$H_{\mu\nu} = p_{\mu} p_{\nu} \frac{1}{2} \left[G_E^2(Q^2) + \frac{Q^2}{4m_p^2} G_M^2(Q^2) \right] \frac{1}{1 + Q^2/4m_p^2} + (q^2 g_{\mu\nu} - q_{\mu} q_{\nu}) \frac{1}{2} G_M^2(Q^2). \quad (2.2)$$

The familiar electric and magnetic form factors $G_E(Q^2)$ and $G_M(Q^2)$ only depend on the squared four-momentum of the exchanged photon $q^2 \equiv -Q^2 < 0$ and are well parametrized by the dipole form

$$G_E(Q^2) = (1 + Q^2/0.71 \text{ GeV}^2)^{-2}, \quad (2.3a)$$

$$G_M(Q^2) = 2.79 G_E(Q^2). \quad (2.3b)$$

The leptonic tensor $L_{\mu\nu}$ does obviously depend on the process considered. Let us denote by p_1 and p_2 the momenta of the incoming electron and the outgoing charged sparticle, respectively, and by $\hat{s}, \hat{t} = (p_1 - p_2)^2$ and \hat{u} the Mandelstam variables of the $e\gamma^* \rightarrow$ sparticles subprocess. For selectron photino production we find

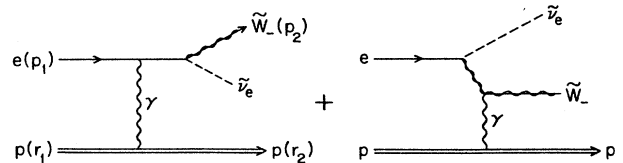


FIG. 2. Feynman diagrams for the process $ep \rightarrow p\tilde{\nu}_e \tilde{W}_-$.

where f_+ describes W -ino–Higgsino mixing.⁴

Note that the $1/Q^4$ dependence of the cross section is spurious; electromagnetic gauge invariance ensures that $L_{\mu\nu}H^{\mu\nu}$ vanishes as Q^2 for $Q^2 \rightarrow 0$. Unlike cases in which the photon is radiated by the electron, in our case the cancellations that ensure this behavior are not so strong to require a special way to write the matrix elements for numerical evaluations. The reason is that the lowest possible Q^2 of the photon is proportional to the squared mass of the emitting particle, which in our case is the proton. Equations (2.1)–(2.5) can thus directly be used for a computer code.

B. The modified equivalent-photon approximation

Unfortunately the exact computation of the total cross sections using Eqs. (2.1)–(2.5) necessitates the evaluation of a four-dimensional phase-space integral. This can become very time consuming if one wants to scan the parameter space of supersymmetry (see Sec. V). We therefore developed a modified equivalent-photon (Weizsäcker-Williams¹⁴) approximation. In this approximation the cross section for $ep \rightarrow pX$ can be written as

$$\sigma(ep \rightarrow pX) = \int_{z_{\min}}^{z_{\max}} f_{\gamma|p}(z) \hat{\sigma}(\gamma e \rightarrow X), \quad (2.6)$$

where $f_{\gamma|p}(z)$ is the density of photons inside the proton carrying the energy fraction z and $\hat{\sigma}$ is the cross section for the production of X in *real* γe scattering, evaluated at a squared center-of-mass-system (cms) energy $\hat{s} = zs$. The relevant expressions for $\hat{\sigma}$ can be found in Refs. 12 and 13.

Note that $f_{\gamma|p}(z)$ cannot be obtained by the well-known¹⁴ form of the photon density inside an electron by just replacing the electron mass with the proton mass; this would overestimate the cross section by a factor of 2 or more, since all form factor effects would be neglected. Instead we used

$$f_{\gamma|p}(z) = \frac{\alpha}{2\pi z} [1 + (1-z)^2] \left[\ln A - \frac{11}{6} + \frac{3}{A} - \frac{3}{2A^2} + \frac{1}{3A^3} \right], \quad (2.7)$$

where $A = 1 + (0.71 \text{ GeV}^2)/Q_{\min}^2$ and

$$Q_{\min}^2 = -2m_p^2 + \frac{1}{2s} [(s + m_p^2)(s - \hat{s} + m_p^2) - (s - m_p^2)\sqrt{(s - \hat{s} - m_p^2)^2 - 4m_p^2\hat{s}}] \quad (2.8)$$

is the minimal possible Q^2 for the production of a final state with squared invariant mass \hat{s} . The result (2.7) has been obtained by integrating over the product of the photon propagator $1/Q^2$ and a typical squared form factor $(1 + Q^2/0.71 \text{ GeV}^2)^{-4}$.

In Figs. 3 and 4 we compare exact and approximate results for selectron-photino and W -ino–sneutrino produc-

tion. One sees that in the former case the error of the approximation is at most 20% for all interesting combinations of parameters, and at most 30% in the latter case. The approximation is thus good enough to perform scans of parameter space, since the overestimate of the total cross section corresponds to a shift in the selectron or chargino mass of 5 GeV or less.¹⁵

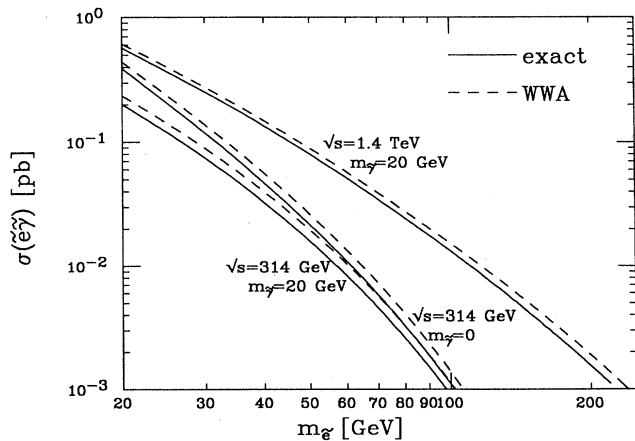


FIG. 3. Total cross section for the reaction $ep \rightarrow p e \gamma$ at $\sqrt{s} = 314 \text{ GeV}$ (HERA) and $\sqrt{s} = 1.4 \text{ TeV}$ (ep collider in the LEP tunnel). The solid curves are the exact results according to Eqs. (2.1)–(2.4), whereas the dashed curves have been obtained with the modified equivalent-photon (Weizsäcker-Williams) approximation, Eqs. (2.6)–(2.8).

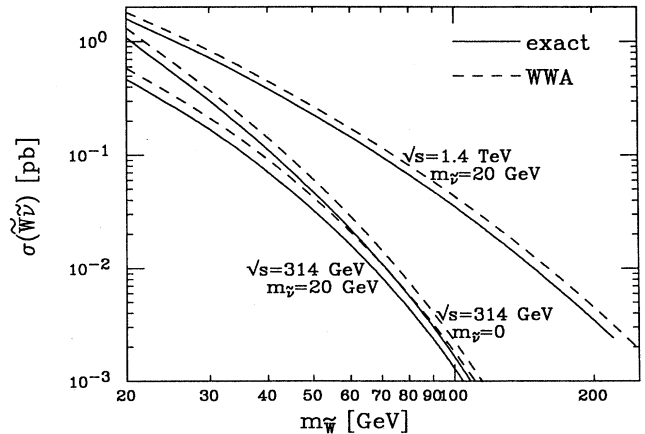


FIG. 4. Total cross section for the process $ep \rightarrow p e \tilde{W}_-$ at $\sqrt{s} = 314 \text{ GeV}$ and $\sqrt{s} = 1.4 \text{ TeV}$ where the chargino is assumed to be a pure W -ino. Exact and approximate results are again shown separately.

III. $\tilde{e}\tilde{Z}_1$ PRODUCTION AT HERA

In this section $\tilde{e} + \tilde{Z}_1$ production with subsequent $\tilde{e} \rightarrow e + \tilde{Z}_1$ decay is discussed in detail for the forthcoming HERA collider ($\sqrt{s} = 314$ GeV). We will assume the \tilde{Z}_1 to be a photinlike state ($\tilde{\gamma}$) which is either stable or decays invisibly into $\tilde{\nu} + \nu$. Since HERA can only probe the region below $m_{\tilde{e}} \simeq 50$ GeV, it is reasonable^{4,16} to assume 100% branching ratio for the $e + \tilde{Z}_1$ decay mode of the selectron. The situation might be more complicated¹⁶ for higher selectron masses, which can be probed, e.g., at the proposed collider using LEP I and the Large Hadron Collider (LEP I \times LHC) with $\sqrt{s} = 1.4$ TeV.

A. Signal

In the process $ep \rightarrow \tilde{\gamma}\tilde{e}p \rightarrow \tilde{\gamma}\tilde{\gamma}ep$ both photinos escape unobserved, and the event thus consists of one hard electron plus missing energy-momentum in the main detector. In addition, the outgoing proton might be detected in the forward proton spectrometer, since it is less energetic than the other beam protons and will thus be bent out of the beam by the bending magnets. The efficiency for this detection has been estimated¹⁷ to be around 50% for a "generic" event, but may well be higher for certain spectacular types of events (as the ones under discussion), since in this case it might be possible to use less severe requirements for the proton detection.

Even if the proton is not detected the signal should be easily recognizable, since the standard-model background is very small. The only physics backgrounds arise from elastic $\nu_e + W^-$ or $e + Z^0$ production with subsequent $W^- \rightarrow e\tilde{\nu}_e$ and $Z^0 \rightarrow \nu\tilde{\nu}$ decays. The corresponding cross sections are estimated^{7,18} to be smaller than 0.01 pb at $\sqrt{s} = 314$ GeV. Furthermore these backgrounds are in principle subtractable, since the total $\nu_e W^-$ and $e + Z^0$ cross sections can be measured, making use of other decay modes of the gauge bosons. This approach might be necessary at LEP I \times LHC, where the SM background reaches ~ 0.1 pb.

In Fig. 5 we show the transverse-momentum (p_{Te}) spectrum of the electron that results from the decay of the selectron. All curves have a pronounced peak at the value p_e^* of the electron momentum in the rest frame of the selectron:

$$p_e^* = \frac{m_{\tilde{e}}^2 - m_{\tilde{\gamma}}^2}{2m_{\tilde{e}}}. \quad (3.1)$$

Note that the suppression of QED background from $ep \rightarrow e\gamma p$ where the γ goes down the beam pipe necessitates a cut

$$p_{Te} \geq E_{e \text{ beam}} \sin \theta_{\text{res}}, \quad (3.2)$$

where θ_{res} is the angle down to which photons can be detected and $E_{e \text{ beam}}$ is the energy of the electron beam. For the ZEUS detector,¹⁷ $\theta_{\text{res}} \simeq 3^\circ$, which leads to a p_{Te} cut at 1.6 GeV. From Fig. 5 it is obvious that such a cut would only affect the signal for very small values of $m_{\tilde{e}} - m_{\tilde{\gamma}}$, below 5 GeV.

Another requirement is, of course, that the electron it-

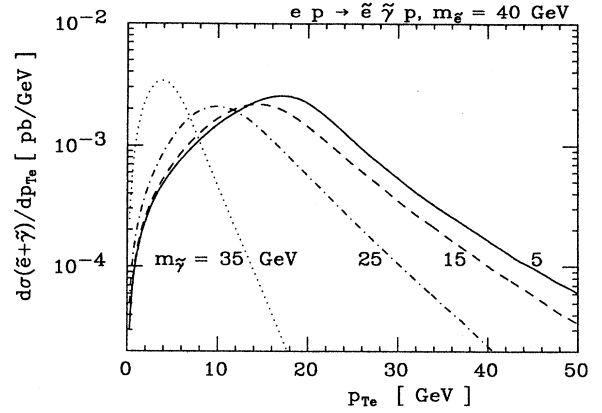


FIG. 5. The transverse-momentum spectrum of the electron that results from \tilde{e} decay in elastic $\tilde{e}\tilde{\gamma}$ events at HERA. Since the transverse momentum of the outgoing proton is very small, this spectrum is practically identical to the missing p_T spectrum. This and all subsequent figures are at HERA energy ($\sqrt{s} = 314$ GeV).

self is not lost in the beam pipe. In Fig. 6 we show the polar-angle distribution of the decay electron in the laboratory frame for $m_{\tilde{e}} = 40$ GeV and various values of $m_{\tilde{\gamma}}$ (θ_e is measured with respect to the proton beam). Obviously a restriction such as $3^\circ \leq \theta_e \leq 176^\circ$ (for the ZEUS detector¹⁷) will not reduce the signal significantly.

The only other visible particle in the signal events is the outgoing, "slow" proton. In Fig. 7 the cross section is shown as a function of the relative energy loss of the proton, $z \equiv (E_p^{\text{in}} - E_p^{\text{out}})/E_p^{\text{in}}$, which is equivalent to the energy of the transmitted photon. All curves clearly show the threshold at

$$z_{\text{min}} = \frac{(m_{\tilde{e}} + m_{\tilde{\gamma}})^2}{s}. \quad (3.3)$$

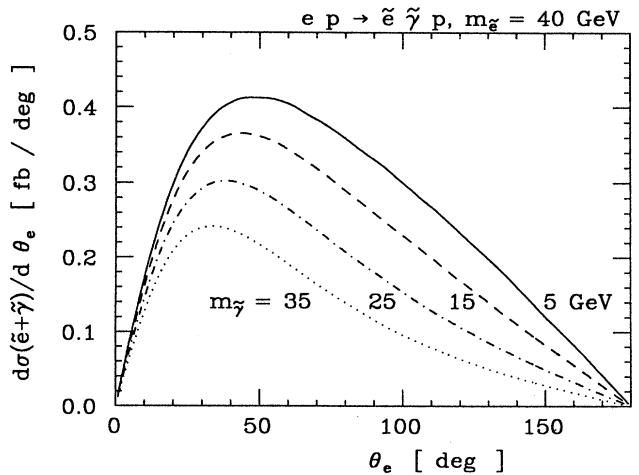


FIG. 6. The polar-angle distribution in the laboratory frame of the decay electron in elastic $\tilde{e}\tilde{\gamma}$ events. $\theta_e = 0$ corresponds to the proton beam direction.

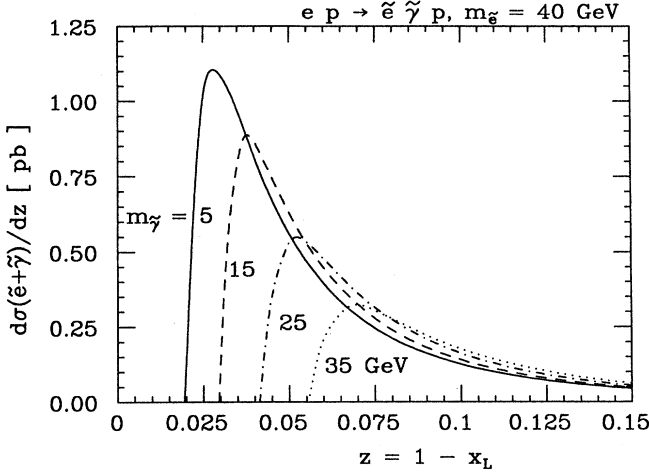


FIG. 7. The elastic $\bar{e}\tilde{\gamma}$ cross section as a function of $z = (E_p^{\text{in}} - E_p^{\text{out}})/E_p^{\text{in}} = E_\gamma/E_p^{\text{in}}$.

The threshold is not quite as pronounced for light photinos. This can most easily be understood in the equivalent-photon approximation. In the threshold region the cross section for the $\gamma e \rightarrow \tilde{\gamma} \bar{e}$ subprocess goes as $1 - m_e^2/\hat{s}^2$ for $m_\gamma = 0$, where $\hat{s} = zs$, whereas in the limit $m_\gamma = m_e$ this cross section is only suppressed by a factor $(1 - 4m_e^2/\hat{s})^{1/2}$, leading to a much steeper threshold behavior.

It is also interesting to note that the curves of Fig. 7 peak at values of z where the detection efficiency for the proton is maximal,¹⁷ around 50% if one uses the “generic” cuts. Recall, however, that in the case under consideration milder requirements might suffice.

Finally we should mention that the transverse momentum of the outgoing proton is typically only 100 MeV, and almost never more than 1 GeV. The reason is, of course, that the form factors (2.3) strongly suppress the cross section at high Q^2 . [Note that $Q^2 \simeq (p_{T_p}^2)/(1-z)$ for $p_{T_p}^2 \gg Q_{\text{min}}^2$; see Eq. (2.8).] These values of the proton transverse momentum are too small to interfere with the proton detection in the forward spectrometer; they also mean that the missing p_T spectrum of the signal events is practically indistinguishable from the p_{Te} spectrum shown in Fig. 5.

B. Event reconstruction

Next we turn to simple methods to determine both m_e and m_γ from a limited number of events.

In principle the transverse-momentum and polar-angle distributions of the decay electron are sufficient for this reconstruction. We have already seen (Fig. 5) that the p_{Te} spectrum peaks near the value p_e^* of the electron momentum in the selectron rest frame, Eq. (3.1). What is more, Fig. 8 shows that the expectation value of p_{Te} is also very close to p_e^* . By generating samples of signal events with a Monte Carlo generator we found that ten events should be enough to determine p_e^* with an error of

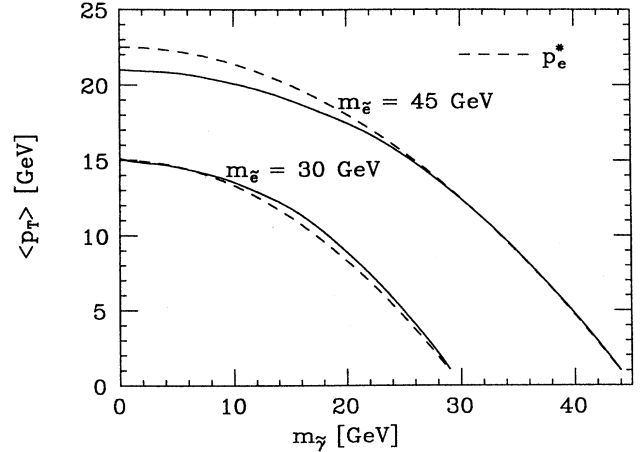


FIG. 8. The average transverse momentum of the decay electron in elastic $\bar{e}\tilde{\gamma}$ events. The value p_e^* of the electron momentum in the selectron rest frame [see Eq. (3.1)] is also shown (dashed curves).

roughly 15%, assuming perfect measurement of p_{Te} .

Figure 6 shows that the angular distribution of the electron has a mild peak in the proton direction, which becomes more pronounced as $m_e + m_\gamma$ increases. This is a purely kinematic effect: larger sparticle masses imply that the proton has to lose more energy, see Eq. (3.3), which in turn leads to a stronger boost of the selectron-photino system into the proton direction. By measuring the angular distribution of the electron one should thus be able to determine $m_e + m_\gamma$.

A much more direct and simpler determination of this sum becomes possible if the energy of the outgoing proton is measured. We have already seen in Fig. 7 that in most events the relative energy loss z of the proton is not much larger than its kinematic minimum z_{min} . The smallest observed z should therefore be a reasonable approximation for z_{min} . Indeed we find that with this simple method one usually overestimates the sum $m_e + m_\gamma$ by less than 5 GeV if 10 fully measured events are observed. (This error increases to about 8 GeV in the somewhat pathologic case $m_\gamma = 0$, due to the different threshold behavior in this case; see our discussion in Sec. III A.) If one combines this measurement with the measurement of $\langle p_{Te} \rangle \simeq p_e^*$ as discussed above, one can determine both m_e and m_γ with an error of around 5–7 GeV, again assuming a sample of 10 fully reconstructed events. Given the simplicity or even crudeness of this method, this is not too bad a result.

This result can certainly be improved by performing a maximum-likelihood fit to the actual data with m_e and m_γ as free parameters. In between these two extremes we have devised a method which does take into account the major correlations between observables, but which still is based on kinematic considerations only. The basic observation is that in the center-of-mass frame of the $e\gamma \rightarrow \bar{e}\tilde{\gamma}$ subprocess the selectron energy E_e is fixed,

$$E_e = \frac{\hat{s} + m_e^2 - m_{\tilde{\gamma}}^2}{2\sqrt{\hat{s}}}, \quad (3.4)$$

and hence the end points E_e^\pm of the electron energy spectrum arising from $\tilde{e} \rightarrow e\tilde{\gamma}$ decay are fixed:

$$E_e^\pm = \frac{m_e^2 - m_{\tilde{\gamma}}^2}{2(E_e \mp p_e)}. \quad (3.5)$$

The end-point energies are a function of the subprocess invariant mass $\sqrt{\hat{s}}$ and of the sum and the difference of the particle masses

$$\sigma = m_e + m_{\tilde{\gamma}}, \quad (3.6a)$$

$$\Delta = m_e - m_{\tilde{\gamma}}. \quad (3.6b)$$

Assuming that the proton momentum is measured in the forward proton spectrometer, \hat{s} is determined for each event. From the complete proton energy spectrum, or more precisely the threshold at $z_{\min} = (m_e + m_{\tilde{\gamma}})^2/s$, the sum of sparticle masses σ will be known as well, and from Eq. (3.5) the only remaining unknown quantity, $\Delta = m_e - m_{\tilde{\gamma}}$, can be isolated, albeit with a twofold ambiguity:

$$\Delta_\pm = \frac{1}{\hat{s} + \sigma^2 \frac{\hat{s}}{E^2} \left[1 - \frac{2E}{\sqrt{\hat{s}}} \right]} \times \left[\sigma \hat{s} \left(\frac{\sqrt{\hat{s}}}{E} - 1 \right) \pm \frac{\sigma \hat{s}}{E} \sqrt{\hat{s} - \sigma^2} \left[1 - \frac{2E}{\sqrt{\hat{s}}} \right]^{1/2} \right], \quad (3.7)$$

where E is either of the two end-point energies. Instead of using the unknown end-point energies E_e^\pm for fixed $\sqrt{\hat{s}}$ one can determine $\Delta_\pm(E)$ where E is the measured electron energy in the subprocess rest frame for any particular event. The resulting Δ_\pm spectra for $m_e = 40$ GeV, $m_{\tilde{\gamma}} = 15$ GeV are shown in Fig. 9. For illustration the exact value $\sigma = 55$ GeV was used in Eq. (3.7). Clearly the Δ_- (Δ_+) spectrum is bounded from above (below) by $m_e - m_{\tilde{\gamma}}$, and even for a small number of events the information contained in these two spectra is a powerful tool to determine the selectron-photino mass difference. When, for a small number of events, $m_e + m_{\tilde{\gamma}}$ is identified with the minimal observed value of $\sqrt{zs} = \sqrt{\hat{s}}$, one often encounters an unphysical overlap of the Δ_+ and Δ_- spectra, which in turn allows a better estimate for the sum of sparticle masses. Using this trick and correcting for the systematic shift to larger $m_e + m_{\tilde{\gamma}}$ values due to the limited statistics we have estimated that for $m_e = 40$ GeV and $m_{\tilde{\gamma}} = 5, 15, 25, 35$ GeV, ten well-reconstructed events allow a reconstruction of m_e with a statistical error of 1.3–1.8 GeV and of $m_{\tilde{\gamma}}$ with a statistical error of 1.2–2.0 GeV (both increasing with decreasing photino mass). Hence even with the observation of only a handful of elastic $\tilde{e}\tilde{\gamma}$ events a rather precise determination of sparti-

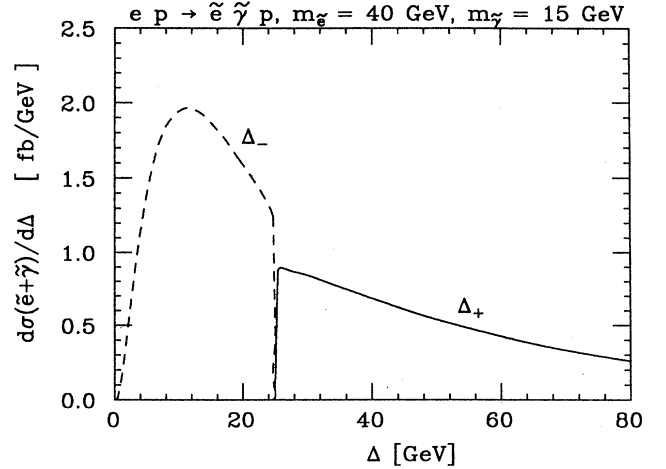


FIG. 9. The elastic $\tilde{e}\tilde{\gamma}$ cross section as a function of Δ_+ and Δ_- as defined in Eq. (3.7).

cle masses appears feasible, with errors which will soon be dominated by the resolution of the detectors.

IV. SIGNALS FROM $\tilde{e}\tilde{Z}_2$ AND $\tilde{\nu}\tilde{W}_-$ PRODUCTION

In this section we discuss the signals for the other two potentially interesting elastic SUSY processes at HERA, the production of a selectron plus the second-lightest neutralino and of an electron sneutrino plus the lightest chargino. Obviously these signals depend crucially on how the produced gauginos decay, which is strongly model dependent. We therefore restrict ourselves to a more qualitative discussion.

A. Selectron-neutralino production

In Sec. III selectron-photino production was discussed in some detail, under the assumption that the photino escapes detection. Here the production of a heavier neutralino is discussed, which will in general decay visibly.

We work within the framework of minimal supersymmetry,¹ where the masses and mixings of the four neutralino and two chargino mass eigenstates are determined by the values of three parameters: The gluino mass $m_{\tilde{g}}$, the supersymmetric Higgsino mass μ , and the ratio $\omega \equiv v_2/v_1$ of the vacuum expectation values of the two neutral Higgs fields (the masses of up-type quarks are proportional to v_2). In general, all of these parameters can be either positive or negative (the physical gluino mass is given by $|m_{\tilde{g}}|$), but for our purposes only the sign of the product $\mu m_{\tilde{g}} \omega$ is relevant.

In general neither of the four neutralino states will be a photino; in this case a factor of $2e^2$ in Eq. (2.4) will have to be replaced by the square of the $e_L \tilde{e}_L \tilde{Z}_i$ or $e_R \tilde{e}_R \tilde{Z}_i$ couplings given in Ref. 19. Note that the couplings are in general different for left- and right-handed electrons. Furthermore the masses of \tilde{e}_L and \tilde{e}_R can also be quite different. In this case one expects the signal cross section to depend strongly on the polarization of the incident electrons.

In Fig. 10 we show total cross sections for the production of all four neutralino states as a function of $m_{\tilde{g}}$, for $m_{\tilde{e}_L} = m_{\tilde{e}_R} = 40$ GeV, $\mu = 50$ GeV, and $\omega = 1.5$. The discontinuities in the curves correspond to level crossings of the neutralino eigenstates; e.g., at $m_{\tilde{g}} \simeq -200$ GeV the state that formerly corresponded to the second heaviest neutralino becomes the heaviest state.

The most remarkable result of Fig. 10 is that \tilde{Z}_1 production is dominant only if $|\mu| \gtrsim \frac{1}{4}|m_{\tilde{g}}|$. Outside this region \tilde{Z}_1 is dominantly a Higgsino and thus couples only weakly to electrons; the cross section for \tilde{Z}_2 production might, however, still be sizable in this region. Since the masses of a Higgsino-like or photino-like state can be approximated by $|\mu|$ and $0.15|m_{\tilde{g}}|$, respectively, \tilde{Z}_2 production will become more important with decreasing $|\mu|$; in the extreme (and unrealistic¹) case $\mu = 0$ the massless \tilde{Z}_1 will never be produced. On the other hand, we find that at HERA energies the cross sections for the production of the two heaviest neutralinos are almost always too small to lead to detectable event rates.

The produced selectron will usually decay into $e + \tilde{Z}_1$ as before, leading to a hard electron. In principle, the \tilde{Z}_2 can undergo two- or three-body decays leading to a $f\tilde{f}\tilde{Z}_1$ final state where f is a quark or lepton. Recall, however, that \tilde{Z}_2 production at HERA will only be interesting if $m_{\tilde{e}} \lesssim 50$ GeV, whereas from the Collider Detector at Fermilab²⁰ (CDF) we now know that squarks are heavier than about 80 GeV. \tilde{Z}_2 -decays via real or virtual sleptons will thus always dominate⁴ over decay modes involving (virtual) squarks, and also over those decays that proceed¹⁹ via W or Z exchange.

The signatures resulting from these leptonic \tilde{Z}_2 decays

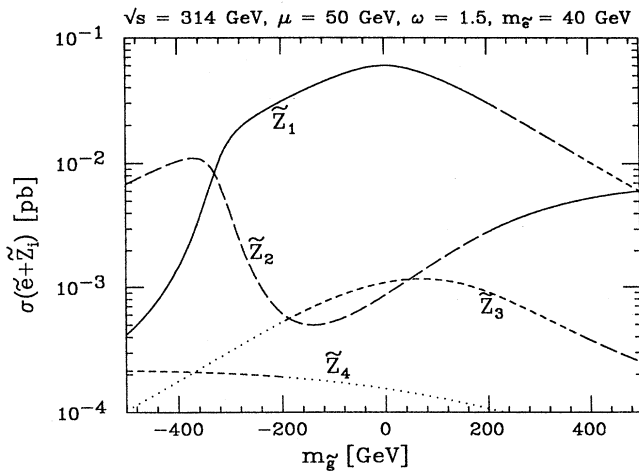


FIG. 10. Total elastic $e\tilde{Z}_i$ cross sections at $\sqrt{s} = 314$ GeV in minimal supersymmetry where all neutralino and chargino masses and mixings are given by μ , $m_{\tilde{g}}$, and ω . Here and in the remaining figures the modified effective-photon approximation has been used. The discontinuities in the curves result from level crossings of the neutralino eigenstates. Degenerate left- and right-handed selectrons are assumed.

are all very clean. If sneutrinos are the lightest sleptons, the \tilde{Z}_2 will decay invisibly, and the signal will be very similar to the one discussed in Sec. III. (Because of the different kinematics, the details of the electron spectrum will, however, be somewhat different.) Otherwise the final state will contain a total of three charged leptons, one electron, and an l^+l^- pair, where $l = e, \mu, \tau$. These three possibilities will occur with (almost) equal rates if slepton masses are (almost) the same for all generations, as expected¹ in minimal supergravity. In addition, the event will have missing p_T . As discussed in Sec. III, the SM background for the electron + \cancel{p}_T signal is very small. There is no $O(\alpha^3)$ SM process that can produce three charged leptons plus missing p_T .

There is still one possibility left, however, that can lead to a hadronic final state: The decay $\tilde{Z}_2 \rightarrow \tilde{Z}_1 H_L^0$, where H_L^0 is the light Higgs boson²¹ of minimal supersymmetry. If the \tilde{Z}_1 is dominantly a Higgsino and \tilde{Z}_2 a gaugino, but not a photino, this decay occurs with full gauge strength.^{19,22} Notice furthermore that the H_L becomes light if either $\omega \rightarrow 1$ (Ref. 21) or the supersymmetry-breaking scale is small,²³ which in our case is indicated by $m_{\tilde{e}} \lesssim 50$ GeV; it thus seems quite likely that this decay channel is open if the $e\tilde{Z}_2$ cross section is sizable. The Higgs boson would decay into a $b\bar{b}$ pair or, if $m_{H_L} < 2m_b$, into $c\bar{c}$ or $\tau^+\tau^-$ pairs, leading to a partly hadronic final state. In this case ordinary deep-inelastic neutral-current events might be a serious background if mismeasurement produces some fake \cancel{p}_T . This might make it necessary to include the detection of the outgoing proton into the event definition, which in turn would reduce the detection efficiency.

B. Sneutrino-chargino production

The signals that emerge from the production of $\tilde{\nu}_e + \tilde{W}_-$ depend crucially on which of these sparticles is the lighter one.

If $m_{\tilde{\nu}_e} < m_{\tilde{W}_-}$, the chargino will undergo the two-body decay $\tilde{W}_- \rightarrow \tilde{\nu}_e e$. If, as in minimal supergravity,¹ the different sneutrino species are almost degenerate in mass, the decays $\tilde{W}_- \rightarrow \tilde{\nu}_\mu \mu$ and $\tilde{W}_- \rightarrow \tilde{\nu}_\tau \tau$ will occur with similar rates. Since in this case the sneutrino is light, it will decay invisibly. Similar to the case of $e\tilde{Z}_1$ production the signal in the main detector thus consists of just one hard lepton. Nevertheless the two cases can easily be distinguished, since μ 's and τ 's can only originate from \tilde{W}_- decays; and even if for some reason $m_{\tilde{\nu}_{\mu,\tau}} \gg m_{\tilde{\nu}_e}$ so that the chargino always decays into an electron, experiments with polarized incident electrons should help to distinguish $e\tilde{Z}_1$ from $\tilde{\nu}_e \tilde{W}_-$ production, since the latter vanishes for right-handed electrons.²⁴

In the opposite case $m_{\tilde{\nu}_e} > m_{\tilde{W}_-}$ the situation is somewhat more complicated. The sneutrino will now dominantly decay into $e + \tilde{W}_-$ (the alternative decay into $\nu + \tilde{Z}_1$ involves smaller couplings). The two charginos will undergo three-body decays into $f\tilde{f}'\tilde{Z}_1$, where f, f' are two quarks or leptons. These decays proceed via \tilde{f}, \tilde{f}' , or W exchange. Since HERA can only probe the re-

gion $m_{\tilde{\nu}_e} \lesssim 70$ GeV one might expect the diagrams with $\tilde{\nu}$ exchange to dominate [recall that $m_{\tilde{g}} \geq 80$ GeV from the CDF (Ref. 20)]; however, these graphs also include the $\tilde{Z}_1 \tilde{\nu} \nu$ vertex, which is very small if \tilde{Z}_1 is dominantly a photino or Higgsino. In minimal supergravity $\omega=1$ implies $m_{\tilde{e}_L} = M_{\tilde{\nu}_e}$, which means that leptonic \tilde{W}_- decays ($\tilde{W}_- \rightarrow l \tilde{\nu}_e \tilde{Z}_1$ with $l=e, \mu, \tau$) that proceed via \tilde{L}_L exchange should dominate in the interesting case $m_{\tilde{\nu}} \lesssim 70$ GeV; in this case the event contains three charged leptons, one of which has to be an electron, and missing p_T —a truly striking signature. However, if $\omega > 1$ one has $m_{\tilde{e}_L} > m_{\tilde{\nu}}$ and hadronic \tilde{W}_- decays become possible. In this case the event contains up to two jets plus one isolated lepton, or up to four jets, in addition to the hard electron + \cancel{p}_T . Only in the last case of only one charged lepton could NC backgrounds be a problem and necessitate the identification of the outgoing proton.

V. DISCOVERY POTENTIAL AT HERA

In this section we address the question of what regions of parameter space of minimal supergravity¹ can be covered by the search for elastic supersymmetry (SUSY) processes at HERA. This will be compared to the reach of the contemporary machines LEP I and Tevatron.

We have already seen (Fig. 10) that the cross sections for $\tilde{e} + \tilde{Z}_i$ production vary strongly if the relevant parameters of the neutralino sector are changed. Because of the occurrence of level crossings these cross sections need not even be continuous functions of the parameters. The sum of all four neutralino cross sections is, however, a smooth function of all relevant parameters.

In Fig. 11 we therefore present lines of constant $\sum_{i=1}^4 \sigma(ep \rightarrow p\tilde{e}\tilde{Z}_i)$ for unpolarized incident electrons, $m_{\tilde{e}_L} = m_{\tilde{e}_R} = 30$ GeV and $\omega=1.5$. We have excluded the region between the dotted curves, where the light chargino is lighter than 25 GeV. Outside this region the total elastic neutralino cross section does not strongly depend on μ or ω ; especially for $\omega\mu m_{\tilde{g}} < 0$ the cross section depends mainly on $m_{\tilde{g}}$ (and, of course $m_{\tilde{e}}$).

We also found the polarization dependence of the total neutralino cross section to be rather mild, as long as we assume the superpartners of left- and right-handed electrons to be degenerate in mass. If the incident electrons are right-handed, the total cross section becomes somewhat bigger for large $|m_{\tilde{g}}|$ and smaller for small $|m_{\tilde{g}}|$. The reason is that for large values of $|m_{\tilde{g}}|$ the SU(2) gaugino is too heavy and the cross section is dominated by the production of the U(1)_Y gaugino, which couples more strongly to e_R than to e_L . [For large $|m_{\tilde{g}}|$ the U(1)_Y and SU(2) gauginos are approximate mass eigenstates, with $m_1 = 0.5m_2$.] If $|m_{\tilde{g}}|$ is small, the SU(2) gaugino components of the produced neutralinos, which couple only to e_L , become important.

In Fig. 12 we show lines of constant $\sigma(ep \rightarrow p\tilde{\nu}_e \tilde{W}_-)$ for unpolarized electrons, $\omega=1.5$ and $m_{\tilde{\nu}_e} = 30$ GeV. Unlike in Fig. 4 we have included the mixing effects of the $e\tilde{W}_-\tilde{\nu}_e$ coupling as predicted⁴ by minimal supergrav-

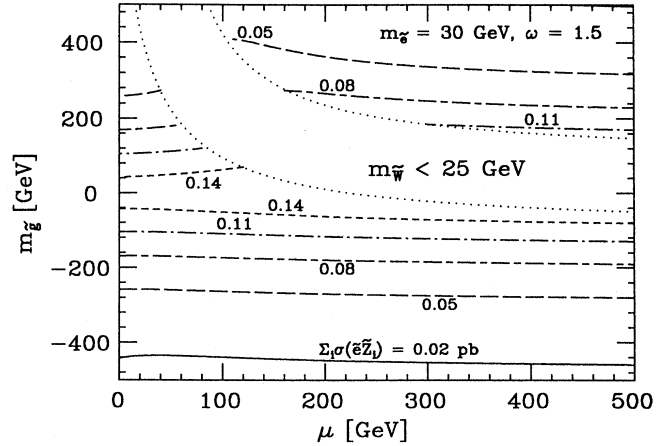


FIG. 11. Lines of constant $\sum_{i=1}^4 \sigma(ep \rightarrow p\tilde{e}\tilde{Z}_i)$ at HERA for $m_{\tilde{e}_L} = m_{\tilde{e}_R}$ and unpolarized incident electrons. The region between the dotted curves was excluded: it corresponds to a light chargino with mass below 25 GeV.

ity for each combination of ω , μ , and $m_{\tilde{g}}$. Nevertheless the cross section is mostly governed by kinematic quantities: The lines of constant cross section more or less coincide with lines of constant $m_{\tilde{W}_-}$. This is not too surprising, since all cross sections considered in this paper depend much more strongly on the mass of the produced charged sparticle than on that of the neutral sparticle, since the charged-sparticle mass does not only enter kinematically via the phase space but also dynamically via the propagator of the relevant u -channel diagram (see Figs. 1 and 2).

Up to now we have assumed the parameters of the scalar and neutralino/chargino sectors to be independent of each other. In this case both neutralino and chargino production can probe the region $|m_{\tilde{g}}| \lesssim 400$ GeV if

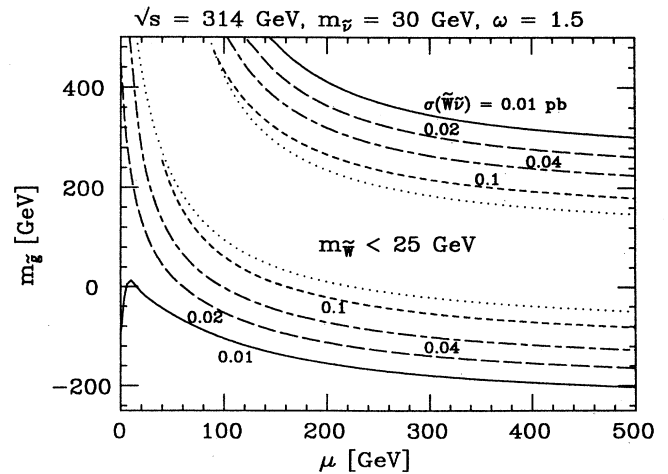


FIG. 12. Lines of constant $\sigma(ep \rightarrow p\tilde{\nu}_e \tilde{W}_-)$ at $\sqrt{s} = 314$ GeV for unpolarized beam electrons.

$m_{\tilde{\nu}} = m_{\tilde{e}} = 30$ GeV, which is close to their experimental lower bounds.²⁵ In minimal supergravity models^{1,26} there are, however, relations between gaugino and sfermion masses. In these models one assumes that all squarks and sleptons have the same mass m_0 at the Planck scale M_P . Similarly, all gauginos are assumed to have the same mass M at M_P . These simple relations are, however, altered by radiative corrections, and at the physically relevant weak scale one has²⁶

$$m_{\tilde{g}} = 3M, \quad (5.1)$$

$$m_{\tilde{e}_R}^2 = m_0^2 + 0.15M^2 - 0.27D, \quad (5.2)$$

$$m_{\tilde{e}_L}^2 = m_0^2 + 0.53M^2 - 0.23D, \quad (5.3)$$

$$m_{\tilde{\nu}}^2 = m_0^2 + 0.53M^2 + 0.5D, \quad (5.4)$$

$$m_{\tilde{q}}^2 \simeq m_0^2 + 7M^2, \quad (5.5)$$

where $D = M_Z^2(1 - \omega^2)/(1 + \omega^2) < 0$ for $\omega > 1$. Equation (5.5) is an approximation for an ‘‘average’’ light-quark flavor and does not hold for \tilde{t} squarks.

The model thus contains four independent parameters that are relevant in our case: m_0 and the three parameters that enter the neutralino/chargino sector. We have already seen, however, that the relevant cross sections become independent of the supersymmetric Higgsino mass μ if $|\mu| \gtrsim 200$ GeV (see Figs. 11 and 12). We therefore chose $\mu = 500$ GeV as a representative value. To be conservative we also chose $\mu M \omega < 0$. We finally take $\omega = 1$, since values close to one are predicted²³ by minimal supergravity if the sparticle spectrum is rather light, as in our case. The solid curves of Fig. 13 show discovery limits from elastic SUSY searches at HERA after one year, corresponding to 200 pb^{-1} . Here we require a total of five elastic SUSY events per year, i.e.,

$$\sum_{i=1}^4 \sigma(ep \rightarrow p\tilde{e}\tilde{Z}_i) + \sigma(ep \rightarrow p\tilde{\nu}_e\tilde{W}_-) = 0.025 \text{ pb}.$$

This number of events will probably not be sufficient for a clear-cut event reconstruction, since in general several types of events will contribute to the total. However, five spectacular events of the types discussed in Secs. III and IV should suffice to show that some new physics has been found.

The perhaps most surprising result of Fig. 13 is that the discovery reach of these elastic SUSY processes is clearly larger than that of the ‘‘classical’’ SUSY processes at HERA, associate slepton + squark production. The dashed curve shows an optimistic⁶ discovery limit for the (in our case) most promising of this class of processes, $\tilde{e}_R\tilde{q}$ production, corresponding to $m_{\tilde{e}_R} + m_{\tilde{q}} = 160$ GeV. The better discovery potential of the elastic processes becomes even more obvious after five HERA years (1 fb⁻¹); see the dot-dashed curve. The reason for this big improvement is that the one-year elastic discovery limits are still far away from the kinematic threshold, unlike the case of slepton-squark production, where the discovery limit after 5 years would only increase by roughly 30%. We thus see that as far as elastic SUSY

searches are concerned luminosity is more important than energy.

Note also that experiments with left- or right-handed incident electrons would probe quite different regions of parameter space. In the former case $\tilde{\nu}\tilde{W}_-$ production is most interesting, which is ideally suited to explore the region of small M , but rather big m_0 , corresponding to rather light \tilde{W}_- but quite heavy $\tilde{\nu}$. For right-handed incident electrons, $\tilde{e}_R\tilde{Z}_1$ production is most promising, which can probe the region of small m_0 , but big M favored by certain ‘‘no-scale’’ models.²⁷ In this region the \tilde{e}_R is fairly light (in fact one has to be careful to avoid²⁸ the region to the left of the dotted line, where the \tilde{e}_R would be stable), while the charginos and neutralinos are rather heavy (except for the \tilde{Z}_1 , of course).

What regions of parameter space can be probed by other colliders? The UA1 Collaboration has already excluded²⁹ the region $m_{\tilde{g}} \lesssim 53$ GeV, corresponding to $M \lesssim 17$ GeV. At the Fermilab Tevatron the CDF Collaboration has announced²⁰ a preliminary bound $m_{\tilde{g}} \gtrsim 90$ GeV, i.e., $M \gtrsim 30$ GeV. For the given combination of parameters a very similar bound can be deduced if $m_{\tilde{W}_-} \gtrsim 40$ GeV, as indicated by studies³⁰ of UA1 monojet events. The Tevatron should eventually be able to probe the region below $m_{\tilde{g}} \simeq 150$ –180 GeV, or $M = 50$ –60 GeV; this would cover most of the region where left-handed polarization is of advantage for elastic SUSY searches at HERA. The forthcoming e^+e^- colliders SLC and LEP can easily probe the region below $m_{\tilde{e}_{L,R}} \simeq 45$ GeV; this is quite similar to the region HERA can probe after one year with right-handed beam electrons. Recall, however, that the region that can be probed by HERA will grow substantially with time, whereas at the e^+e^- machines

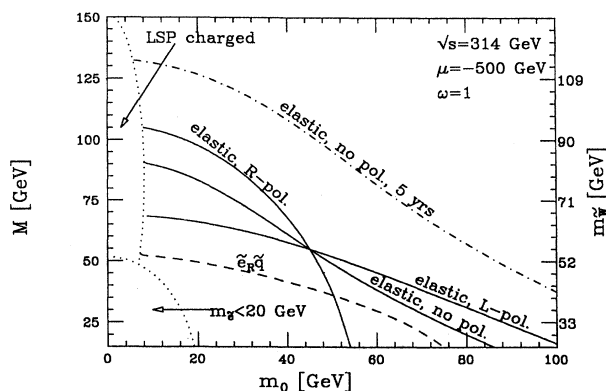


FIG. 13. Discovery limits at HERA within the framework of minimal supergravity where all relevant scalar masses are given by m_0 , M , and ω ; see Eqs. (5.1)–(5.5). The solid (dot-dashed) lines are curves of constant $\sum_{i=1}^4 \sigma(ep \rightarrow p\tilde{e}\tilde{Z}_i) + \sigma(ep \rightarrow p\tilde{\nu}\tilde{W}_-) = 0.025$ (0.005) pb, corresponding to 5 events/year (5 events/5 years), for different polarizations of the beam electrons. The dashed line shows the discovery limit of the best of the ‘‘classic’’ SUSY processes at HERA, $ep \rightarrow \tilde{e}_R\tilde{q}X$, and corresponds to $m_{\tilde{e}_R} + m_{\tilde{q}} = 160$ GeV. The region to the left of the dotted curves are excluded for the indicated reasons.

the sensitive region can only be increased appreciably if the beam energy is increased, as at LEP II.

VI. SUMMARY AND CONCLUSIONS

In this paper we have discussed the elastic production of supersymmetric particles at ep colliders, such as HERA at DESY, via the reactions $ep \rightarrow p\tilde{e}\tilde{Z}_i$ and $ep \rightarrow p\tilde{\nu}\tilde{W}_-$. The main advantages of these production mechanisms are a potentially high-mass reach and very clean final states. The main disadvantage is the smallness of the corresponding cross sections, which are not only of order α^3 , but further suppressed by the form factors of the proton as discussed in Sec. II. In Sec. II we also presented a modified equivalent-photon approximation that includes form-factor effects and works almost as well as the original effective-photon approximation for e^+e^- colliders.

In Sec. III it was shown that ten fully measured $\tilde{e}\tilde{Z}_1$ events where the selectron decays into $e + \tilde{Z}_1$ and the two neutralinos escape detection are enough to determine both $m_{\tilde{e}}$ and $m_{\tilde{Z}_1}$ with a *statistical* error of 2 GeV or less. Since we assumed left- and right-handed selectrons to be degenerate in mass, and did not allow for the contamination of the event sample either by background processes (which should, however, not contribute more than one or two events) or by other supersymmetric processes such as $\tilde{\nu}_e\tilde{W}_-$ production with subsequent $\tilde{W}_- \rightarrow \tilde{\nu}_e e$ decay, our simulation cannot be considered to be fully realistic. However, it clearly demonstrates that the measurement of the momentum of the outgoing proton in a forward proton spectrometer is indeed very helpful.

In Sec. IV signals from $\tilde{e}\tilde{Z}_2$ and $\tilde{\nu}_e\tilde{W}_-$ production were discussed in a more qualitative manner. We found that the \tilde{Z}_2 decays either invisibly or leptonically, giving rise to $e + \cancel{p}_T$ and $e + l^+l^- + \cancel{p}_T$ signals ($l = e, \mu, \tau$) which are practically free of background, unless the $\tilde{Z}_2 \rightarrow \tilde{Z}_1 H_L$ decay is allowed, H_L being the light neutral Higgs boson of minimal supersymmetry. Since the H_L will decay ha-

dronically, standard-model deep-inelastic neutral-current events with fake missing p_T might become a problem if the outgoing proton is not detected. Similarly, $\tilde{\nu}_e\tilde{W}_-$ production leads to an $l^- + \cancel{p}_T$ signature if $m_{\tilde{\nu}_e} < m_{\tilde{W}_-}$, and to $e + 4l + \cancel{p}_T$, $e + l^+l^- + 2 \text{ jets} + \cancel{p}_T$, or $e + 4 \text{ jets} + \cancel{p}_T$ signatures if $m_{\tilde{\nu}_e} > m_{\tilde{W}_-}$ (some of the jets may coincide, so that events with a smaller number of jets are also possible).

In Sec. V we found that, at least within the framework of minimal supergravity models, these elastic SUSY processes can probe a larger region of parameter space than the "classic" SUSY reactions at ep colliders, $ep \rightarrow e\bar{q}X$ and $ep \rightarrow \tilde{\nu}qX$. They enable HERA to compete with the contemporary machines LEP I and Tevatron after one year already. Furthermore, since the one-year discovery limits are still far away from the kinematic limit, the discovery reach at HERA is expected to grow much more rapidly in time than that of LEP I and Tevatron. We thus see that as far as elastic SUSY searches are concerned, luminosity is more important than energy.

It is sometimes claimed that ep colliders combine the worst properties of e^+e^- and pp or $p\bar{p}$ colliders. However, in the elastic SUSY processes discussed in this paper the cleanliness and reconstructability of e^+e^- -events are combined with the potentially high-mass reach of $p\bar{p}$ colliders, thus leading to a harmonic marriage of purely leptonic and hadronic colliders.

ACKNOWLEDGMENTS

We thank the organizers of the Snowmass '88 workshop where this work was initiated. We also gratefully acknowledge helpful discussions with X. Tata, W. Smith, and D. Reeder. This research was supported in part by the University of Wisconsin Research Committee with funds granted by the Wisconsin Alumni Research Foundation, and in part by the U.S. Department of Energy under Contract No. DE-AC02-76ER00881.

¹For recent reviews, see H. P. Nilles, Phys. Rep. **110**, 1 (1984); P. Nath, R. Arnowitt, and A. Chamseddine, *Applied N=1 Supergravity*, ICTP Series in Theoretical Physics (World Scientific, Singapore, 1984); H. E. Haber and G. L. Kane, Phys. Rep. **117**, 75 (1985).

²G. 't Hooft, in *Recent Developments in Gauge Theories*, proceedings of the Cargèse Summer Institute, Cargèse France, 1979, edited by G. 't Hooft *et al.* (NATO Advanced Study Institute—Series B: Physics, Vol. 59) (Plenum, New York, 1980).

³H. Baer and E. L. Berger, Phys. Rev. D **34**, 1361 (1986); **35**, 406(E) (1987); E. Reya and D. P. Roy, Z. Phys. C **32**, 615 (1986).

⁴For a review, see M. Chen, C. Dionisi, M. Martinez, and X. Tata, Phys. Rep. **159**, 201 (1988).

⁵S. K. Jones and C. H. Llewellyn Smith, Nucl. Phys. **B217**, 145 (1983); P. R. Harrison, *ibid.* **B249**, 704 (1985); A. Bartl, H. Fraas, and W. Majerotto, *ibid.* **B297**, 479 (1988).

⁶H. Komatsu and R. Rückl, Nucl. Phys. **B299**, 401 (1988).

⁷G. Altarelli, G. Martinelli, B. Mele, and R. Rückl, Nucl. Phys. **B262**, 204 (1985).

⁸H. Komatsu and R. Rückl, in *Proceedings of the Workshop on Physics at Future Accelerators*, La Thuile, Italy, 1987, edited by J. H. Mulvey (CERN Report No. 87-07, Geneva, Switzerland, 1987).

⁹M. Drees and D. Zeppenfeld, University of Wisconsin Report No. MAD/PH/438, 1988 (unpublished).

¹⁰There are also inelastic contributions where the proton is transformed into a baryon resonance (Δ, N^*, \dots); they were however found to be quite small in K. Hagiwara, S. Komamiya, and D. Zeppenfeld, Z. Phys. C **29**, 115 (1985), where the production of excited electrons was investigated. We will thus neglect them here.

¹¹K. Hidaka, H. Komatsu, and R. Ratcliffe, Nucl. Phys. **B304**, 417 (1988).

¹²M. K. Gaillard, L. Hall, and I. Hinchliffe, Phys. Lett. **116B**,

- 279 (1982); T. Kobayashi, and M. Kuroda, *ibid.* **134B**, 271 (1984).
- ¹³J. A. Grifols and R. Pascual, *Phys. Lett.* **135B**, 319 (1984); G. Eilam and E. Reya, *ibid.* **145B**, 425 (1984); **148B**, 502(E) (1984).
- ¹⁴C. F. Weizsäcker, *Z. Phys.* **88**, 612 (1934); E. J. Williams, *Phys. Rev.* **45**, 729 (1934). For a more recent review of the equivalent-photon approximation, see H. Terazawa, *Rev. Mod. Phys.* **45**, 615 (1973).
- ¹⁵It is amusing to note that our modified effective-photon approximation for a real proton with form factors actually works *better* than the standard Weizsäcker-Williams approximation (WWA) if the proton were pointlike [i.e., $G_E(Q^2)=G_M(Q^2)=1$]. The reason for the rather poor quality of the WWA in this idealized world is the large (compared to m_e) proton mass: $\ln(\hat{s}/m_p^2)$ is typically only about 7.5 at HERA, so that nonlogarithmic terms are still quite important.
- ¹⁶H. Baer, A. Bartl, D. Karatas, W. Majerotto, and X. Tata, University of Wisconsin Report No. MAD/PH/422, 1988 (unpublished).
- ¹⁷ZEUS Collaboration, ZEUS detector technical specification, DESY report (unpublished).
- ¹⁸H. Neufeld, *Z. Phys. C* **17**, 145 (1983).
- ¹⁹H. Baer, D. A. Dicus, M. Drees, and X. Tata, *Phys. Rev. D* **36**, 1363 (1987).
- ²⁰J. Freeman, talk presented at the 7th Topical Workshop on Proton-Antiproton Collider Physics, Fermilab, 1988 (unpublished).
- ²¹K. Inoue, A. Kakuto, H. Komatsu, and H. Takeshita, *Prog. Theor. Phys.* **67**, 1889 (1982); R. A. Flores and M. Sher, *Ann. Phys. (N.Y.)* **148**, 95 (1983).
- ²²J. F. Gunion and H. E. Haber, *Nucl. Phys.* **B272**, 1 (1986).
- ²³M. Drees, M. Glück, and K. Grassie, *Phys. Lett.* **159B**, 118 (1985).
- ²⁴This might be problematic if $m_{\bar{e}_R} \gg m_{\bar{e}_L}$, since in this case $\bar{e}\bar{Z}_1$ production will also be very small for right-handed polarized electrons. Note, however, that in minimal supergravity one always has $m_{\bar{e}_R} \lesssim m_{\bar{e}_L}$.
- ²⁵R. Ansari *et al.*, *Phys. Lett. B* **195**, 613 (1987).
- ²⁶L. E. Ibañez and C. Lopez, *Nucl. Phys.* **B233**, 511 (1984); A. Lahanas, D. V. Nanopoulos, and M. Quiros, *ibid.* **B236**, 438 (1984); L. E. Ibañez, C. Lopez, and C. Muñoz, *ibid.* **B256**, 218 (1985).
- ²⁷For a review, see A. Lahanas and D. V. Nanopoulos, *Phys. Rep.* **145**, 1 (1987).
- ²⁸S. Wolfram, *Phys. Lett.* **82B**, 65 (1979); C. B. Dover, T. K. Gaisser, and G. Steigman, *Phys. Rev. Lett.* **42**, 1117 (1979); D. A. Dicus and V. Teplitz, *ibid.* **44**, 218 (1980).
- ²⁹C. Albajar *et al.*, *Phys. Lett. B* **198**, 261 (1987).
- ³⁰H. Baer, K. Hagiwara, and X. Tata, *Phys. Rev. Lett.* **57**, 294 (1986); *Phys. Rev. D* **35**, 1598 (1987); A. Chamseddine, P. Nath, and R. Arnowitt, *Phys. Lett. B* **174**, 393 (1986).